ACTA ACUSTICA UNITED WITH ACUSTICA
Vol. 93 (2007) 976 – 990

Influence of temporal resolution of meteorological and traffic data on long-term average sound levels

Timothy Van Renterghem, Dick Botteldooren
Ghent University, Department of Information Technology, Sint-Pietersnieuwstraat 41, 9000 Gent, Belgium.
Timothy.Van.Renterghem@intec.Ugent.be

Summary
A theoretical study is conducted to investigate the impact of different time-averaging approaches with regard to meteorological conditions (influencing sound propagation), traffic intensity patterns, and correlation between them, on calculated noise levels. The indicators L_{den} and L_{night}, prescribed by the European Environmental Noise Directive for noise mapping, are of main interest. Sound propagation over flat ground from a long, straight highway is simulated, for receiver distances ranging from 50 m to 2000 m. Detailed, meteorological data from a tower (located near Mol, Belgium), for a full year, is used. An extended database containing yearly-averaged hourly traffic counts is available. Detailed sound propagation calculations are made with the Green's Function Parabolic Equation method, accounting for the refractive state of the atmosphere and range-dependent ground effect. The imprecision introduced by averaging meteorological conditions and traffic intensities over time, and by not fully accounting for the temporal correlation between them, may result in an underestimation up to 20 dB(A) for one-day L_{den} values, using this particular meteorological data set. For yearly-averaged values, the imprecision may reach 3 dB(A). For L_{night}, very similar conclusions could be drawn. Multiple linear regression analysis is used to rank the factors that contribute to the imprecision. This led to the conclusion that the decrease in accuracy resulting from different averaging approaches is mainly proportional to the variability in the refractive state of the atmosphere over a 24 hour-period. The type of traffic intensity profile may intensify this error up to 10 dB(A). The use of meteorological data, statistically-averaged over the year, results in a small loss in accuracy compared to calculating noise levels for every hour of the year and averaging the result afterwards. The error introduced by the approach used to average meteorological condition and traffic intensity over the day is not affected by this.

PACS no. 43.28.Fp, 43.28.Js

1. Introduction

The European Environmental Noise Directive 2002/49/EC prescribes the use of the noise indicators L_{den} and L_{night} for noise mapping and reporting to the European Union. L_{den} is defined as

$$L_{\mathrm{den}} = 10\log_{10}\left(\frac{12}{24}10^{L_{\mathrm{day}}/10} + \frac{4}{24}10^{(L_{\mathrm{evening}}+5)/10} + \frac{8}{24}10^{(L_{\mathrm{night}}+10)/10}\right). \quad (1)$$

where L_{day}, L_{evening} and L_{night} are the A-weighted long-term average sound levels determined over respectively the day period (12 hours, by default from 7.00h till 19.00h), the evening period (4 hours, by default from 19.00h till 23.00h) and the night period (8 hours, by default from 23.00h till 7.00h). Sound pressure levels in the evening period are 'penalised' with 5 dB(A), those at night with 10 dB(A). These penalties partly account for the difference in perceived noise annoyance during different parts of the day caused by varying sensitivity to environmental noise, changing activities, and expectations.

Noise maps for road traffic are often based on the output of traffic models. Most traffic models are developed to describe traffic intensity at peak hours, with the purpose of performing congestion analysis [1]. Information on diurnal and seasonal traffic fluctuations is often missing. As a result, it is important to estimate the error introduced by using less frequent or averaged traffic data to calculate long-term average equivalent sound pressure levels.

In addition, both traffic intensity data and attenuation data show a typical diurnal pattern. Traffic intensity on highways usually peaks in the morning and evening, corresponding to rush hours. Favourable and unfavourable sound propagation conditions are often linked to different periods of the day as well. At night and in the early morning, temperature inversion often occurs, resulting in an increase of sound pressure level at distant receivers. During

Received 8 March 2007,
accepted 18 August 2007.

the day, the atmosphere is usually unstable, resulting in upward refraction of sound and decreased sound pressure levels. Wind speed is often higher during the day. Ignoring this correlation between the diurnal pattern in traffic intensity and sound propagation condition could increase the imprecision caused by a lack of sufficiently detailed traffic data.

In an effort to quantify the above mentioned sources of imprecision in calculating long term average noise indicators, we theoretically studied the effect of gradually decreasing temporal resolution in both meteorological and traffic data. The study is based on a highly detailed meteorological dataset for a single year. Sound propagation from a long, straight road is modeled, for receivers at a distance of up to 2 km. The Green's Function Parabolic Equation method (GFPE) is used. The GFPE is a wave-based sound propagation model accounting in detail for the refraction of sound. The Parabolic Equation method yields accurate predictions of long-term L_{den} levels. In [2], measurements and numerical predictions were compared for the case of sound propagation from a highway towards receivers at a distance of 1115 m over flat terrain (Ladenburg II experiment). The measurement duration was 32 days. Discrepancies between measurements and simulations were limited to only 0.5 dB(A).

By combining GFPE with the detailed meteorological data, sound propagation conditions are obtained on a highly detailed, temporal scale. The combination of these propagation conditions with hourly traffic counts yields the reference value for L_{den} and L_{night}. By subsequent simplification of the calculations by using averages over different periods, insight is gained in the imprecision that the lack of detailed traffic information may introduce. Since it is rather uncommon to have a detailed meteorological dataset like the one used in this study, the impact of using statistically averaged meteorological data is quantified as well.

A preliminary, less detailed study [3] was performed in the framework of Work Package 2 of the IMAGINE project. This work package focused on the requirements for traffic models to produce accurate noise maps. A detailed, meteorological dataset, during two 20 day-periods was used in that study. The emission from a single point source was considered.

The paper is organized as follows. Section 2.1 describes the geometrical set-up and the calculation methodology. The detailed Harmonoise source model is used, and is addressed in section 2.2. Parameters related to the GFPE method are given in section 2.3. The meteorological data set is described in detail in section 3.1, and it is indicated how this information is used to model refraction by the atmosphere in the GFPE model. Information on the traffic database can be found in section 3.2. Section 4 shows how the computational cost can be largely reduced. The temporal averaging approaches are described in section 5. Results are shown and discussed in section 6. Distinction is made between calculations using the actual meteorological data (section 6.1), and calculations that make use of statistically-averaged data (section 6.2). Finally, conclusions are drawn.

2. Calculation methodology

2.1. General

L_{den} and L_{night} levels are calculated at receivers near a long, straight, hypothetical highway. Different configurations are considered. The highway can be oriented either from North to South or from East to West. For the N–S highway, receivers are placed on a line orthogonal to the road, both in eastern and western direction. For the E–W highway, receivers are placed in northern and southern direction. Receiver distances, orthogonal to the roads, are 50 m, 100 m, 500 m, 1000 m, and 2000 m. The ground surface between source and receiver is grassland.

The noise emission from the highway traffic is modelled by a number of point sources. An equi-angular distribution of point sources is chosen. This means that the discretisation of the road is finest near the line of the receivers. The constant angular interval $\Delta\zeta$ is 7.5 degrees. The maximum angle between the receiver line and the line connecting the furthest source point and the receiver point, ζ_{max}, equals 75 degrees. The maximum source-receiver distance is then 7700 m, for the receiver at 2000 m, orthogonal to the road.

The calculation procedure involves the following steps. First, the sound pressure level relative to free field sound propagation is calculated with the GFPE model, for each point source (at two source heights, see section 2.2) and receiver combination. This is done for the 10-minute averaged meteorological parameters (see section 3.1), for the full year, and for the four different configurations described above. Three frequencies per one third octave band are considered, ranging between 50 Hz and 5000 Hz. In section 4, it is indicated how this large amount of calculations can be strongly reduced.

In a next step, the total attenuation for all source receiver pairs is calculated by accounting for geometrical divergence of sound and atmospheric absorption, following ISO 9613-1 [4]. The 10-minute averaged total attenuation data is reduced to hourly attenuation data by energetically averaging over time.

The sound pressure level at the receiver is then calculated as the source power minus the total attenuation, for each one-third octave band. The total A-weighted sound pressure level at a receiver is the incoherent, energetic sum of the contributions of all point sources. Each point source contribution has its own weight because of the equi-angular distribution. The Harmonoise source model uses two source heights (see section 2.2). Contributions from these two sources are summed incoherently as well.

In a final step, integration in time is performed to obtain equivalent sound pressure levels. These form the base of the actual L_{den} and L_{night} calculations. The different approaches for averaging in time are discussed in section 5. Differences in L_{den} and L_{night}, arising from these approaches, will indicate the importance of the temporal correlation between traffic data and sound attenuation data.

2.2. Source description

The Harmonoise source model is used [5]. The number of calculations is reduced by only simulating light vehicles. Such vehicles can be represented by two (incoherent) point sources: The first one is placed at a height of 0.01 m above the road surface, and the second one at a height of 0.30 m. For each source height, separate GFPE calculations are needed. The first source point is associated with rolling noise, the second one with engine noise. 80% of the rolling noise source power obtained from the Harmonoise model should be attributed to the lowest point source, 20% to the highest source point. The engine source power on the other hand is attributed for 80% to the source at 0.30 m, and for 20% to the source at 0.01 m.

A passenger car with two axles is assumed. For each source height, a horizontal and vertical directivity function is available. These depend on the emitted sound frequency and on the vertical and horizontal angle between the source and the receiver location. For each point source, a matching directivity is calculated. The vehicles are assumed to drive at constant speed. Rolling noise is corrected for the temperature of the road. We focus on a common dense asphalt concrete (DAC) top layer, with a temperature correction coefficient of 1 dB/10 °C (air temperature). During colder periods, there will be an increase in the rolling noise emission. The Harmonoise road source model does not include frequency dependent temperature corrections. Tyre corrections, aging and wetness of the road, and regional corrections are not considered. Detailed information and background information on the Harmonoise road source model can be found e.g. in [5].

2.3. GFPE calculations

An axi-symmetric Green's Function Parabolic Equation model is used, as described in [6] and [7]. The GFPE model is used to calculate sound pressure levels at the receiver, relative to free field sound propagation.

The GFPE method has a number of important advantages:

- GFPE allows one to use large step sizes in horizontal direction, which are limited by the inhomogeneity of the atmosphere rather than by the sound wavelength. The maximum acceptable range step varies roughly between 5 to 50 times the wavelength in case of a refracting atmosphere [7]. Since we are aiming at receivers at 2 kilometers orthogonal to the highway, and for typical traffic noise (including relatively high frequencies), the use of large step sizes is an important advantage.
- The computational cost of GFPE is based mainly on the efficiency of the FFT algorithm, and very fast FFT algorithms are available.
- The effective sound speed profiles may contain upward and downward refracting parts.
- Locally reacting, range-dependent impedance planes can be used to model reflection from the ground.

The road surface is modeled as a rigid plane. The grassland is modeled by a complex, frequency-dependent impedance with the one-parameter model of Delany and Bazley [8]. A value for the effective flow resistivity of 200 kPas/m^2 is considered appropriate to model grassland. At 10 m from the road axis, the transition from the rigid road to the grassland is made.

The vertical grid spacing is one tenth of the wavelength, while the horizontal grid spacing is chosen to be 10 times the wavelength with the exception that a variable horizontal propagation step is allowed to exactly reach the position of the impedance jump and the receiver positions.

The presence of a source close to the ground might result in a decrease in accuracy when using a standard Gaussian starting function in the PE model, especially at low frequencies. The approach described in [9] is therefore used. A column of complex pressures is calculated at limited distance from the source with an analytical model, ignoring meteorological effects, and the PE calculation starts from this location.

Near the upper limit of the computational domain, an absorbing layer with a thickness of 150 times the wavelength is applied to simulate an unbounded atmosphere. Inside this layer, an imaginary term is added to the wave number equal to $\mathrm{i}A_t(z - z_t)^2/(z_M - z_t)^2$, where z is the height, z_t is the height where the absorbing layer starts, and z_M is the top of the computational domain. The optimum choice of the constant coefficient A_t depends on frequency and lies between 0 and 1 [10].

3. Datasets

3.1. Meteorological dataset

The meteorological data was recorded on a tower near the city of Mol, in Belgium. Measurements during the year 1997 are available, as 10-minute averages. Wind speed was measured at 5 heights (at 24 m, 48 m, 69 m, 78 m, and 114 m above the ground). Air temperature was measured at 5 heights as well (8 m, 24 m, 48 m, 78 m, and 114 m above the ground). Wind direction was measured at 3 heights (24 m, 69 m, and 114 m above the ground). Relative humidity data is available from a nearby observation point, on an hourly base, at 1.5 m above the ground.

For the analysis in this paper, only days having at least a single 10-minute period with complete observations in each hour could be used. This requirement resulted in a 60-day missing period during summer.

Frequency distributions of the wind speed at 24 m, wind direction at 24 m, air temperature at 8 m, relative humidity at 1.5 m, and the temperature difference between 114 m and 8 m (normalized over 100 m) are shown in Figure 1. The mean wind speed at 24 m equals 3.1 m/s. Wind is blowing most of the time from the south-western direction (225 degrees), and second most from the eastern direction (near 90 degrees). The atmosphere is most often slightly unstable to neutral.

The GFPE model uses the effective sound speed approach. The effective sound speed at the measured heights

can be calculated using air temperature, wind speed, and wind direction:

$$c_{\text{eff}} = \sqrt{\kappa RT} + u_{SR}(z), \tag{2}$$

In this formula, κ is the ratio of the specific heat capacities at constant pressure and constant volume, which equals 1.4 in air. R is the gas constant of dry air and equals 287 J/(kg K). The dependency of the sound speed on water vapor fraction in air is neglected. The wind speed along the source-receiver line is given by $u_{SR}(z)$, and may have a positive or negative sign. When the wind is blowing orthogonal to the source-receiver line, its contribution to the effective sound speed is zero. The propagation of sound emitted by different stretches of roads to the same observation point experiences different wind components within a single meteorological observation. The wind direction at 24 m (the lowest observation point) is most relevant since sources and receivers are located close to the ground.

Meteorological parameters are measured at a single horizontal location. The refractive state of the atmosphere is therefore assumed to be constant between the locations of source and receiver.

The PE method needs the effective sound speed profiles with high vertical resolution. Since observations are available on a limited number of heights, a linear-logarithmical (effective) sound speed curve will be fitted on the data,

$$c_{\text{eff}} = a_0 + a_{\text{lin}} + a_{\log} \log \frac{z + z_0}{z_0}. \tag{3}$$

The parameters a_{lin} and $a_{\log}$ can be related to the physical parameters of theoretical-empirical flux-profile relationships for the case of a flat, homogeneous terrain [11]. Good fits on meteorological tower measurements were obtained in [12], notwithstanding the limited number of parameters in equation (3). This type of effective sound speed profile is recommended by the Harmonoise project.

Meteorological measurements at low heights (< 8 m) are not available in our database. Air temperature observations close to the ground could improve the fit on the above described sound speed profile, especially under conditions of ground-based temperature inversion. On the other hand, the observation point at 114 m above the ground limits the need for extrapolation of wind speed and air temperature data. This is an important advantage, since meteo at this height is relevant for sound propagation up to a receiver at 2 km from the source.

For each meteorological observation, the parameters a_0, a_{lin} and $a_{\log}$ were estimated, for each combination of source and receiver locations, in all configurations. The absolute value of the effective sound speed profile is not important to model refraction of sound. Therefore, the sound speed profiles are determined by the parameters a_{lin} and $a_{\log}$ only. A value of a_0 equal to 340 m/s is assumed in all cases. The roughness length z_0 was chosen to be 0.1 m, which is typical for agricultural land with scattered obstacles. Because of the large amount of combinations, the a_{lin}–$a_{\log}$ parameter space is reduced to a number

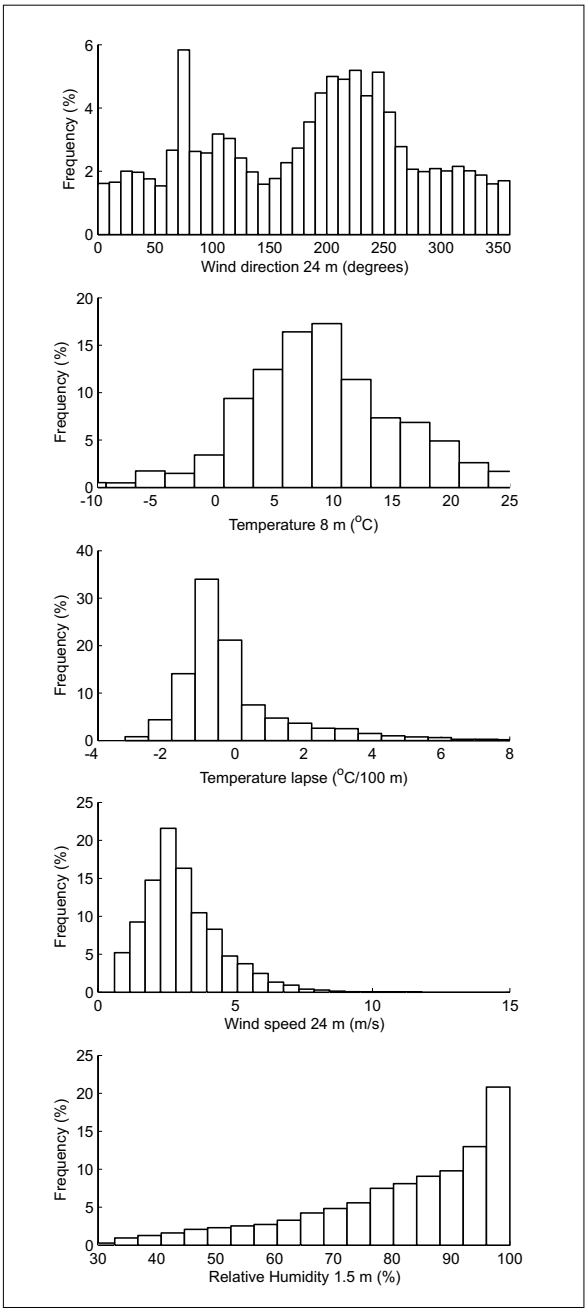

Figure 1. Histograms of some parameters in the meteorological dataset. Wind direction at 24 m, wind speed at 24 m, air temperature at 8 m, relative humidity at 1.5 m, and the temperature lapse are shown.

of classes. Similar a_{lin}–$a_{\log}$ combinations result in similar sound propagation conditions. Class widths of 0.01/s and 0.1 m/s are used for respectively a_{lin} and $a_{\log}$, and calculations will be performed for the centre values of each class. This resulted in about 1500 different classes, as is shown in Figure 2. A number of calculations were performed for the centre values of classes, using smaller class widths (namely 0.0075/s and 0.075 m/s). The differences in sound pressure level between corresponding classes in

both approaches were not significant at a propagation distance of 2000 m. Thus the selected resolution of 0.01/s and 0.1 m/s was assumed sufficient for the reference calculations in this paper.

When considering statistically-averaged meteo classes (see section 6.2), this number of classes will be reduced to 25 [2], since this detail in available data is unlikely in practical applications.

Relative humidity and air temperature are used to calculate the frequency-dependent atmospheric absorption. The influence of atmospheric pressure is limited and is therefore neglected. The magnitude of the atmospheric absorption is calculated as αr, where α is the absorption coefficient following ISO 9613-1 [4] and r is the distance travelled by the direct sound ray between source and receiver. Atmospheric absorption changes from hour to hour in the reference calculations.

The acoustical characteristics of the ground between the edge of the road and the receivers will change with meteorological condition. As is shown e.g. in [13] and [14], an increase in soil moisture content causes an increased flow resistivity, resulting in an acoustically harder ground. Soil humidity data was unfortunately not present in the meteorological dataset. In case of a snow-covered ground on the other hand, an acoustically much softer ground is expected. The change of soil characteristics over time is not considered in this study because of a lack of sufficient data.

3.2. Traffic intensity dataset

The traffic data consists of yearly-averaged hour-by-hour traffic intensities, for the different days of the week separately. The database is based on traffic counts at 285 locations along highways in Flanders, Belgium. A large variety of traffic intensity profiles are available, ranging from profiles with distinct rush-hour peaks in the morning and in the evening, to profiles with a rush-hour peak only in the morning or only in the evening, as well as more uniform distributions of traffic intensity over a 24-hour period. Day-by-day or seasonal variations in traffic intensity can not be deduced from the database. Traffic composition and traffic speed are not known. This information is however not essential for the analysis made in this paper.

4. Improving computational efficiency

4.1. Maximum frequency to be calculated at each distance

To calculate L_{den} and L_{night}, total A-weighted sound pressure levels are needed. Computational efficiency can be drastically increased by a priori limiting the maximum propagation distance that needs to be considered for each frequency to reach a given accuracy.

The importance of the contributions of different frequencies to the total A-weighted sound pressure level at each distance is estimated. To do this, different values of atmospheric absorption are combined with typical traffic noise spectra of light vehicles corresponding to driving speeds ranging from 70 to 130 km/h. Atmospheric absorption is mainly determined by air temperature and relative humidity. In this analysis, air temperature ranged from −10 °C to 30 °C, relative humidity ranged from 30% to 90%. Frequencies where the level is 15 dB(A) below the total A-weighted sound pressure level were considered to be unimportant. Excess attenuation either by the presence of the ground or by the refractive state of the atmosphere is neglected in this analysis which makes it a fast pre-scan.

The maximum and minimum frequencies to be considered at each distance, for the different combinations described above, are shown in Figure 3. In a conservative approach, the maximum of the maximums and the minimum of the minimums are used as the frequency band of interest at each distance. Figure 3 shows that very low frequencies should not be considered at short distances, because

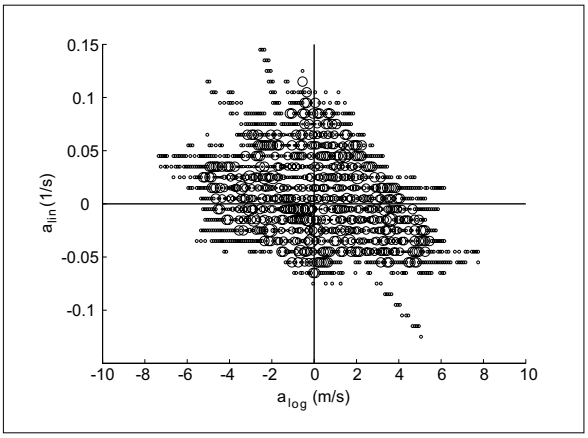

Figure 2. Scatter plot of the a_{lin}–a_{log} classes used for the reference calculations in this paper. The centres of the circles represent the class midpoints. The radius of each circle is proportional to the number of data points in each class.

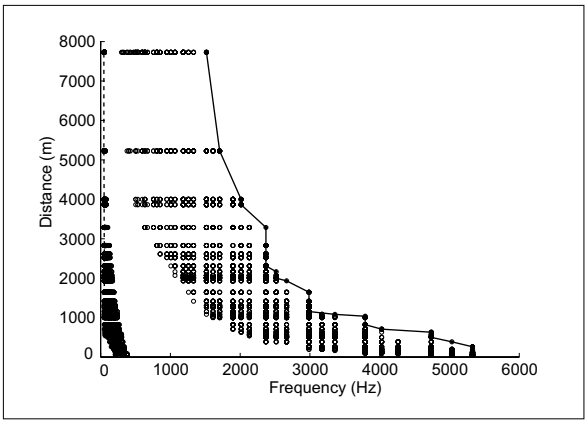

Figure 3. The open circles indicate the maximum and minimum frequencies that should be considered (taking into account the −15 dB(A) criterion) at different source receiver distances, for different combinations of the magnitude of atmospheric absorption, and for A-weighted traffic spectra. The maximum and minimum frequencies that are used in the GFPE calculations are shown with respectively the full line and the dashed line.

of their limited importance in the traffic spectrum, and because of the application of the A-weighting filter. Since the computational cost of the PE method at these frequencies is very low, they were not omitted from the calculations.

Computational efficiency benefits especially from limiting the propagation distance at high frequencies. The one-third octave band of 5000 Hz is only relevant until 600 m, while the largest frequency to be calculated near 7700 m is reduced to 1500 Hz.

To validate the choice of the 15 dB(A) cut off, the same analysis was repeated for a 20 dB(A) cut off. As a consequence, the maximum distance to be reached for each frequency increased, and the computational cost increased drastically. For a number of a_{lin}–$a_{\log}$ pairs, with values in each of the four quadrants of the parameter space, total A-weighted sound pressure levels were calculated with frequency ranges obtained with both cut offs. The results differed only at a few propagation distances, and to a very small degree (at maximum 0.1 dB(A)). The cut off value of 15 dB(A) was therefore considered to result in sufficiently accurate frequency ranges of importance while keeping calculation effort modest.

4.2. Sound propagation in turbulent atmosphere

In the case of an upward refracting atmosphere, turbulent scattering into the acoustic shadow zone that is formed, becomes important. Neglecting this effect often results in unrealistically large attenuations. A standard approach to account for turbulent scattering consists in simulating sound propagation through a number of turbulent realisations of the atmosphere (see e.g. [15]). The ensemble average of all these realisations follows statistical laws. To have statistically stable results however, at least 50 realisations of the turbulent atmosphere need to be taken into account. As a result, computing times increase drastically. The phase-screen method presented by Di *et al.* [16] is an alternative for the many-realisation approach.

Based on experiments, it was found that the sound pressure level relative to free field sound propagation stays more or less constant in the acoustical shadow zone formed by an upward refracting atmosphere [17, 18]. This constant value depends on the geometry of the problem and on the strength of the turbulence. A value of −25 dB is common in outdoor sound propagation literature. Truncating the sound pressure level relative to free field comes at no additional computational cost and is therefore chosen.

The combination of a source very close to the ground, an acoustically rather soft ground, and an upward refracting atmosphere result in a monotonically decreasing sound pressure level with distance once the distance from the source is sufficient. Therefore, further calculations can be stopped at this frequency, once the sound pressure level relative to free field sound propagation equals −25 dB. This limiting value is then used for the remaining distances.

Besides scattering of sound into an acoustic shadow zone, turbulence causes phase and amplitude fluctuations, leading to a reduced depth of the interference minima between direct and ground-reflected waves [10]. For sound propagation above a finite-impedance ground however, the difference in destructive inference between a turbulent and non-turbulent atmosphere is much less pronounced than above rigid ground [15]. Furthermore, strong turbulence is usually accompanied by large wind speeds and temperature gradients. Numerical simulations in [10] show that the effect of turbulence on interference minima is limited in case of downward refraction. Hence this effect is not accounted for in this study, to keep computational cost within reasonable limits.

4.3. Equivalent sound propagation conditions

Different road orientations, wind speeds, and wind directions could result in the same a_{lin}–$a_{\log}$ class for some combinations of source points and receiver points. Even a period with wind in a homogeneous atmosphere and a windless period in an inhomogeneous atmosphere could possibly result in the same effective sound speed curve. It is clear that equivalent sound propagation conditions appear, although configurations could be completely different. This can be exploited to increase computational efficiency. During the GFPE calculations, the relative sound pressure level is recorded at all distances between the source points on the highways and the receivers that appear in the discretised problem (i.e. 21 source points times 5 receivers) for each a_{lin}–$a_{\log}$ class. Afterwards, for each source-receiver combination, the relative sound pressure levels at the correct propagation distance are retrieved from this dataset depending on the actual meteorological situations.

5. Approaches for averaging over time

The most accurate L_{den} value, indicated as $L_{\text{den}}^{(\text{ref})}$, is based on calculations that combine the emission at a certain hour with the corresponding attenuation for this same hour. In this way, the coupling between the traffic noise emission and sound attenuation is accounted for to a large extent. These calculations serve as a reference for less accurate estimates of L_{den}.

It is assumed that all vehicles on the road are identical. The emitted source power at source point j for hour i is then expressed as

$$L_{w,j,i} = 10\log_{10}\left(w_j N_i 10^{L_w/10}\right), \tag{4}$$

where N_i equals the number of vehicles in hour i, and L_w is the frequency-dependent and time-independent, acoustical source power of a single vehicle. Because of the equiangular distribution of source points over the road, each point source has its own weight w_j, given by

$$w_j = \frac{\tan(\zeta_j - \Delta\zeta/2) - \tan(\zeta_j + \Delta\zeta/2)}{2\tan(\zeta_{\max} + \Delta\zeta/2)}, \tag{5}$$

where z_j is the angle between the receiver line and the line between the source point j, located in the centre of

Table I. Formulas to determine $L_{\mathrm{den}}^{(\mathrm{ref})}$, $L_{\mathrm{den}}^{(1)}$, $L_{\mathrm{den}}^{(2)}$, $L_{\mathrm{night}}^{(\mathrm{ref})}$ and $L_{\mathrm{night}}^{(1)}$. $L_{w,j,i}$ is the acoustical source power emitted by road segment j during hour i and is given by equation (4), L_w is the acoustical source power of a single vehicle, $A_{j,i}$ is the transmission from source point j to the receiver in hour i, and N_i is the number of vehicles in hour i. For clarity, the formulas are not fully simplified.

$L_{\mathrm{day},j}^{(\mathrm{ref})} = 10\log_{10}\left(\frac{1}{12}\sum_{i=7}^{18} 10^{(L_{w,j,i}-A_{j,i})/10}\right)$	$L_{\mathrm{evening},j}^{(\mathrm{ref})} = 10\log_{10}\left(\frac{1}{4}\sum_{i=19}^{22} 10^{(L_{w,j,i}-A_{j,i})/10}\right)$	$L_{\mathrm{night},j}^{(\mathrm{ref})} = 10\log_{10}\left(\frac{1}{8}\sum_{i=23}^{6} 10^{(L_{w,j,i}-A_{j,i})/10}\right)$
$L_{w,\mathrm{day},j}^{(1)} = L_w + 10\log_{10}\left(\frac{1}{12} w_j \sum_{i=7}^{18} N_i\right)$	$L_{w,\mathrm{evening},j}^{(1)} = L_w + 10\log_{10}\left(\frac{1}{4} w_j \sum_{i=19}^{22} N_i\right)$	$L_{w,\mathrm{night},j}^{(1)} = L_w + 10\log_{10}\left(\frac{1}{8} w_j \sum_{i=23}^{6} N_i\right)$
$A_{\mathrm{day},j}^{(1)} = -10\log_{10}\left(\frac{1}{12}\sum_{i=7}^{18} 10^{-A_{j,i}/10}\right)$	$A_{\mathrm{evening},j}^{(1)} = -10\log_{10}\left(\frac{1}{4}\sum_{i=19}^{22} 10^{-A_{j,i}/10}\right)$	$A_{\mathrm{night},j}^{(1)} = -10\log_{10}\left(\frac{1}{8}\sum_{i=23}^{6} 10^{-A_{j,i}/10}\right)$
$L_{\mathrm{day},j}^{(1)} = L_{w,\mathrm{day},j}^{(1)} - A_{\mathrm{day},j}^{(1)}$	$L_{\mathrm{evening},j}^{(1)} = L_{w,\mathrm{evening},j}^{(1)} - A_{\mathrm{evening},j}^{(1)}$	$L_{\mathrm{night},j}^{(1)} = L_{w,\mathrm{night},j}^{(1)} - A_{\mathrm{night},j}^{(1)}$
$L_{w,\mathrm{day},j}^{(2)} = L_w + 10\log_{10}\left(\frac{1}{12} 0.7 w_j \sum_{i=0}^{23} N_i\right)$	$L_{w,\mathrm{evening},j}^{(2)} = L_w + 10\log_{10}\left(\frac{1}{4} 0.2 w_j \sum_{i=0}^{23} N_i\right)$	$L_{w,\mathrm{night},j}^{(2)} = L_w + 10\log_{10}\left(\frac{1}{8} 0.1 w_j \sum_{i=0}^{23} N_i\right)$
$A_{\mathrm{day},j}^{(2)} = A_{\mathrm{day},j}^{(1)}$	$A_{\mathrm{evening},j}^{(2)} = A_{\mathrm{evening},j}^{(1)}$	$A_{\mathrm{night},j}^{(2)} = A_{\mathrm{night},j}^{(1)}$
$L_{\mathrm{day},j}^{(2)} = L_{w,\mathrm{day},j}^{(2)} - A_{\mathrm{day},j}^{(2)}$	$L_{\mathrm{evening},j}^{(2)} = L_{w,\mathrm{evening},j}^{(2)} - A_{\mathrm{evening},j}^{(2)}$	$L_{\mathrm{night},j}^{(2)} = L_{w,\mathrm{night},j}^{(2)} - A_{\mathrm{night},j}^{(2)}$
$L_{\mathrm{den},j}^{(ref,1,2)} = 10\log_{10}\left(\frac{12}{24} 10^{L_{\mathrm{day},j}^{(ref,1,2)}/10} + \frac{4}{24} 10^{(L_{\mathrm{evening},j}^{(ref,1,2)}+5)/10} + \frac{8}{24} 10^{(L_{\mathrm{night},j}^{(ref,1,2)}+10)/10}\right)$		
$L_{\mathrm{den}}^{(ref,1,2)} = \sum_j 10^{L_{\mathrm{den},j}^{(ref,1,2)}/10}$	$L_{\mathrm{night}}^{(ref,1)} = \sum_j 10^{L_{\mathrm{night},j}^{(ref,1)}/10}$	

road segment j, and the receiver point. The values for the constant angular interval, $\Delta\zeta$, and the maximum angle between the receiver line and the line connecting the furthest source point and the receiver point, $\zeta_{\max}$, that are used in this study, are given in section 2.1.

Since this section focuses on averaging procedure in time, summations over spatial indices will be omitted in the remainder of this section. An overview of the formulas that will be used for the different averaging approaches is given in Table I.

A first approximate calculation (further indicated as *approach 1*) assumes that traffic data is known only as an average for the (default) day period, evening period and night period. The calculation of $L_{\mathrm{den}}^{(1)}$ is a combination of the overall source powers during day, evening and night ($L_{w,\mathrm{day}}^{(1)}$, $L_{w,\mathrm{evening}}^{(1)}$, and $L_{w,\mathrm{night}}^{(1)}$) with the overall attenuations during these three periods ($A_{\mathrm{day}}^{(1)}$, $A_{\mathrm{evening}}^{(1)}$, and $A_{\mathrm{night}}^{(1)}$) respectively. For the comparison in this paper, these attenuation values are obtained by energetically averaging the hourly attenuations in the relevant periods of the day. The calculation of $L_{w,\mathrm{day}}^{(1)}$, $L_{w,\mathrm{evening}}^{(1)}$, and $L_{w,\mathrm{night}}^{(1)}$ is based on the average of the hourly traffic counts in the relevant periods. In the case of a uniform traffic intensity profile ($N_i = cst$), the approximate solution is exactly equal to the reference calculation.

For the second approximate calculation (further indicated as *approach 2*), it is assumed that only the total traffic intensity in a full 24-hour period is known. The $L_{\mathrm{den}}^{(2)}$ calculation needs however at least traffic intensity in each of the 3 periods, in order to apply the 5-dB and 10-dB factors. Therefore, the total traffic intensity is spread over the day period, the evening period, and the night period, based on the recommendations of the Good Practice Guide [19]: 70% of the total 24-hour traffic intensity should be attributed to the day period, 20% to the evening period, and 10% to the night period if detailed information is lacking. The second approach differs from the first one only by the fact that in the first approach, the actual division of the traffic intensity over the three periods is known. The calculation of overall attenuations during these three periods stays the same. The flow chart in Figure 4 gives an overview of the various calculation approaches.

Note that in the averaging approaches, all acoustical energy produced by the source, and all attenuation of acoustical energy is conserved. Differences arise solely from neglecting correlations in time between source power and attenuation data.

The influence of the temporal resolution of traffic data on L_{night} is considered separately. For the reference calculation $L_{\mathrm{night}}^{(\mathrm{ref})}$, the emission at each night hour is combined with the corresponding attenuation at that hour. The approximate solution $L_{\mathrm{night}}^{(1)}$ uses a single, overall night emission and a single, overall night attenuation.

6. Results and discussion

6.1. Actual meteorological data

Noise indicators calculated using the actual meteorological data, i.e. calculating noise levels for each hour or period of the day, throughout a full day or year, and averaging results afterwards, will be referred to as calculations on a sequential base, and are indicated with the subscript "SEQ". Large underestimations of one-day L_{den} values are possible when using approach 1 or 2. In Figure 5, the errors introduced by using approach 1, relative to the reference calculation ($= L_{\mathrm{den,1day,SEQ}}^{(1)} - L_{\mathrm{den,1day,SEQ}}^{(ref)}$), are shown by means of box plots. The data points in these boxplots

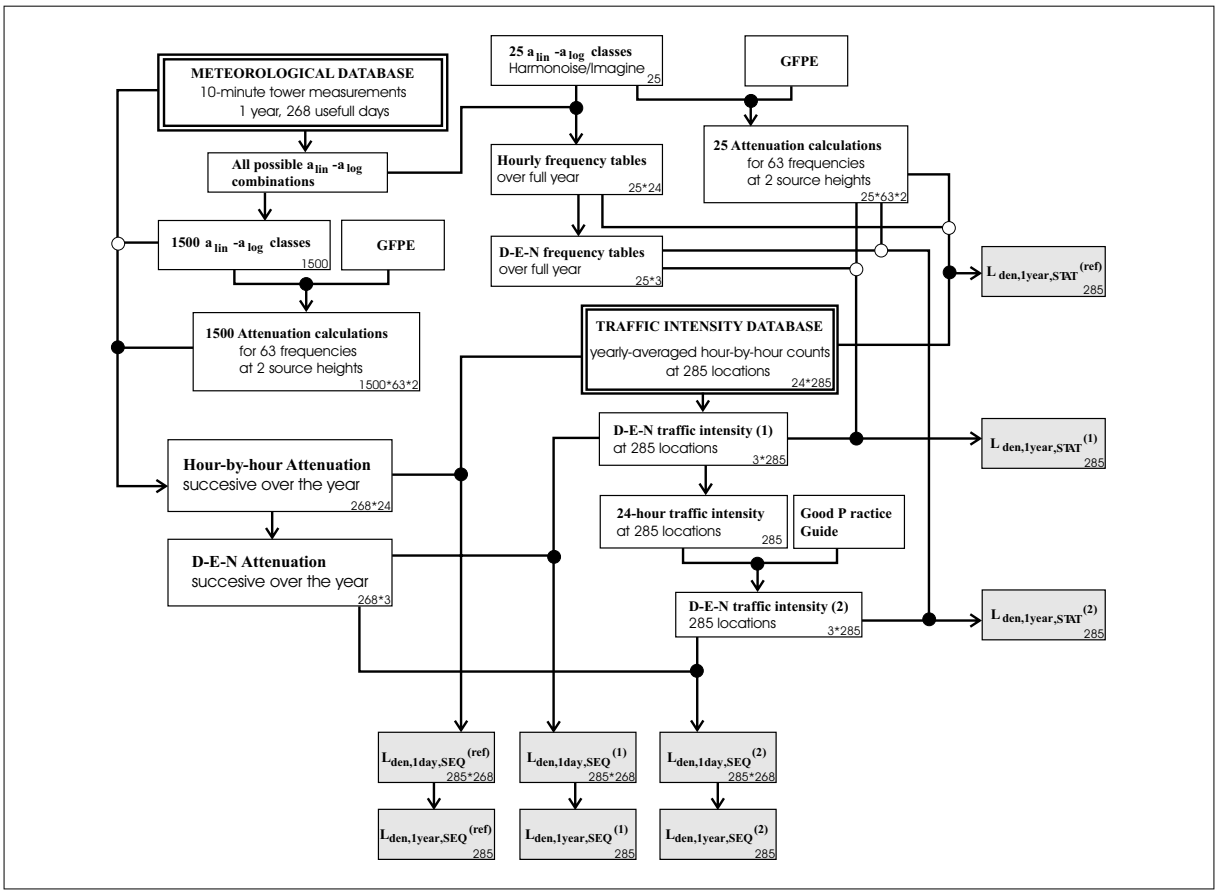

Figure 4. Schematic representation of the calculation methodology and the averaging approaches used in this study, for both statistical (indicated with the subscript "STAT") and non-statistical (sequential, indicated with the subscript "SEQ") meteorological data. For simplicity, L_{den} values at a single receiver, resulting from a single source point, are considered.

are all possible combinations of days with available meteo data with all available traffic intensity profiles (= 268 times 285 values). A separate box plot is used for each receiver distance. Although the data itself can strictly speaking not be considered as a continuous distribution, the use of box plots is an interesting way to present the results in a concise way. The (middle) horizontal line in the box indicates the median of the data. The box is closed by the first and third quartile. The whiskers extend to 1.5 times the interquartile distance above the maximum value inside the box, and to 1.5 times the interquartile distance below the minimum value inside the box. Data points that fall outside these limits are indicated with the plus-signs.

With increasing distance, the absolute value of the maximum errors become larger, and saturate once a distance of 1000 m is reached. The maximum difference between one-day $L^{(1)}_{\mathrm{den,1day,SEQ}}$ and $L^{(\mathrm{ref})}_{\mathrm{den,1day,SEQ}}$ is more than 15 dB(A). Although there are some prominent wind directions in the meteorological dataset, the results shown in Figure 5 depend only marginally on highway and observer orientations. The errors introduced by using approach 2 give quite similar box plots (not shown). The main difference is the magnitude of the maximum error, which reaches 20 dB(A).

One-night $L^{(1)}_{\mathrm{night,1night,SEQ}}$ values, relative to the reference $L^{(\mathrm{ref})}_{\mathrm{night,1night,SEQ}}$, show similar behaviour. The maximum error found here is 23 dB(A), at a distance of 2 km. The variability of the errors for short-term L_{den} and L_{night} values is similar.

It can be concluded that a sufficient temporal resolution is needed to prevent the possibly strong underestimations of short-term (daily) L_{den} and L_{night} values.

Errors introduced on yearly L_{den} by using average traffic intensities are much smaller. The large errors that were found for the one-day L_{den} values are now averaged out to an important degree. In Figure 6, box plots of $L^{(1)}_{\mathrm{den,1year,SEQ}} - L^{(ref)}_{\mathrm{den,1year,SEQ}}$ for the 285 traffic profiles are shown. Figure 7 shows equivalent box plots for $L^{(2)}_{\mathrm{den,1year,SEQ}} - L^{(\mathrm{ref})}_{\mathrm{den,1year,SEQ}}$. Approach 1 leads to underestimations of up to 1.5 dB(A) at 2 km, approach 2 to underestimations of up to 3 dB(A). The influence of variability in diurnal traffic intensity profiles is very small in approach 1, but becomes more important in approach 2. The median decreases with distance in both approaches, and reaches about −1 dB(A) at 2 km. The behaviour of the error on yearly L_{night} values is very similar to the error related to L_{den} for approach 1. As a result, it can be concluded that

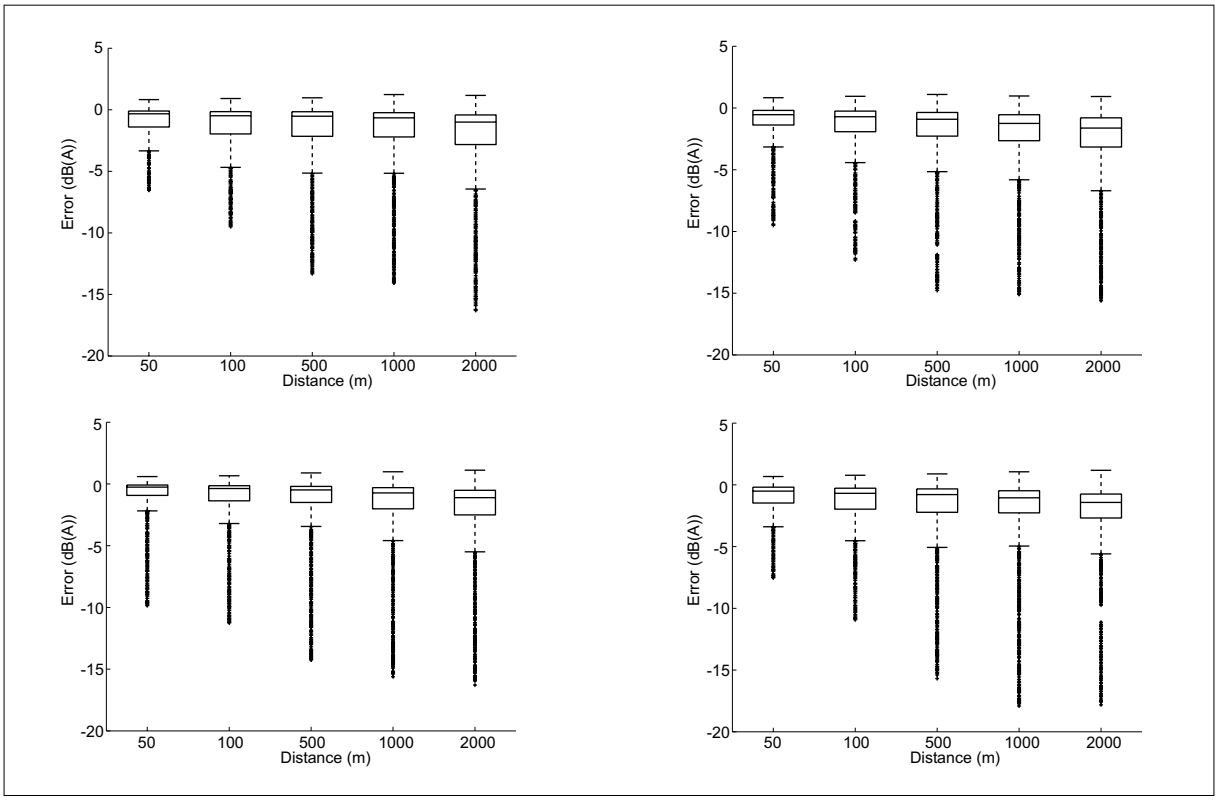

Figure 5. Errors on one-day L_{den} values by using approach 1, relative to the reference calculations ($= L^{(1)}_{\mathrm{den,1day,SEQ}} - L^{(\mathrm{ref})}_{\mathrm{den,1day,SEQ}}$). The data points forming the box plots are all days in combination with all traffic intensity profiles. Top left: Highway N–S, receivers E; top right: Highway N–S, receivers W; bottom left: Highway E–W, receivers N; bottom right: Highway E–W, receivers S.

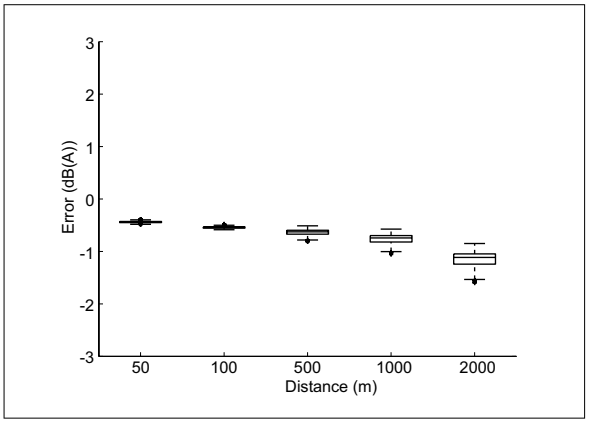

Figure 6. Errors on yearly L_{den} values by using approach 1, relative to the reference calculations ($= L^{(1)}_{\mathrm{den,1year,SEQ}} - L^{(\mathrm{ref})}_{\mathrm{den,1year,SEQ}}$). The data points forming the box plots are the different traffic intensity profiles. The other configurations gave similar box plots and are therefore not shown.

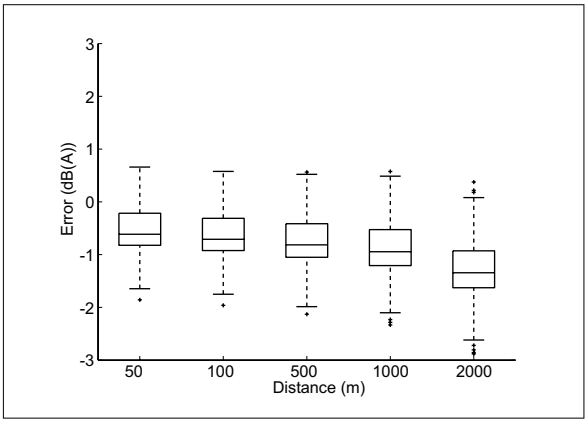

Figure 7. Errors on yearly L_{den} values by using approach 2, relative to the reference calculations ($= L^{(2)}_{\mathrm{den,1year,SEQ}} - L^{(\mathrm{ref})}_{\mathrm{den,1year,SEQ}}$). The data points forming the box plots are the different traffic intensity profiles. The other configurations gave similar box plots and are therefore not shown.

the detailed course of traffic intensity over time has less influence on the indicators considered when the integration period is long enough. Note that day-to-day variations in diurnal traffic intensity profiles are not explicitly accounted for in this analysis, since only yearly-averaged hour-by-hour traffic counts were available.

In the results above, temporal averaging over longer periods, as well as an increase in propagation distance, lead to increasingly stronger underestimates of average sound pressure levels. Periods with high traffic intensity and at the same time downward refracting sound propagation conditions contribute a lot to L_{den}. With increasing

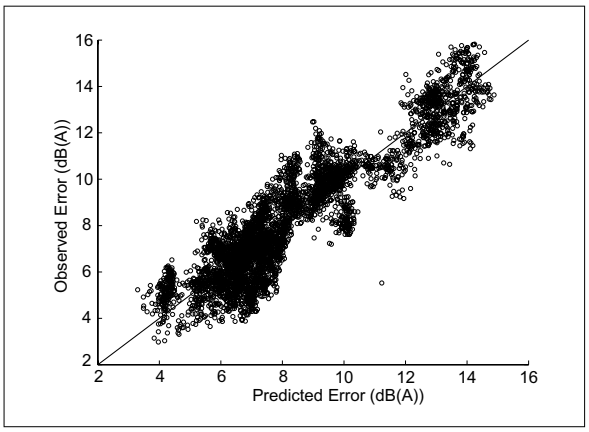

Figure 8. The error predicted by the multiple linear regression model including interactions, versus the error observed for one-day L_{den} values, using averaging approach 1 (= $L^{(1)}_{den,1day,SEQ} - L^{(ref)}_{den,1day,SEQ}$). Days resulting in maximum errors, larger than 5 dB(A), were selected.

distance, the effect of downward refraction becomes more prominent, leading to an increased contribution from these periods. Averaging these correlations out gives stronger underestimates and the effect is more pronounced when the averaging period is longer.

Multiple linear regression analysis helps to reveal the main parameters responsible for the error when using a certain diurnal averaging approach. The traffic parameters that will be used for this statistical analysis are the total traffic intensity over the day, the evening, and the night, relative to the total traffic intensity over the three periods. The meteorological parameters are reduced to the mean values of a_{lin} and a_{log} during the day, the evening and the night. These 9 parameters form the base for the prediction of the error by using approach 1 for averaging over time. We are especially interested in the relative importance of the chosen parameters for situations resulting in the largest errors, for one-day L_{den} values. For deriving the model, days resulting in maximum errors larger than 5 dB(A), for a highway with N–S orientation, and receivers at 2 km in easterly direction are selected. This approach was chosen since it is observed that during these days, the influence of the traffic intensity profile is important. On days where the maximum errors are limited on the other hand, traffic data has hardly any influence.

Pair wise combinations of these 9 parameters are considered as well, that are further indicated as interaction terms. This means that the multiple linear regression model has at maximum 46 parameters (see further), including a constant term.

A regression model with interaction terms is able to explain 84% (i.e. R^2) of the variability in the above described error. The null hypothesis that all coefficients in our linear model are zero could be rejected at the 99.99% level. The predicted errors on one-day L_{den} values (= $L^{(1)}_{den,1day,SEQ} - L^{(ref)}_{den,1day,SEQ}$) are plotted against the observed values in Figure 8. Most pairs follow the diagonal quite well. Analysis of the standardized residuals shows that the quality of the model is similar in all cases and the differences between observed and predicted values follow closely a Gaussian distribution (not shown).

Table II. Retained parameters for the multiple linear regression model, to predict the error $L^{(1)}_{den,1day,SEQ} - L^{(ref)}_{den,1day,SEQ}$, introduced by using averaging approach 1. Days with maximum errors larger than 5 dB(A) were selected for this analysis. The parameters are ranked by their standardized coefficients SD.

parameter	SD	parameter	SD
$a_{log,evening}a_{lin,day}$	−7.67	$a_{lin,night}a_{log,night}$	0.73
$a_{log,evening}a_{log,night}$	−6.56	$I_{evening}I_{night}$	0.83
$a_{lin,night}$	−2.69	$a_{lin,night}I_{night}$	0.88
$a_{lin,day}a_{lin,night}$	−2.67	$a_{lin,evening}I_{evening}$	1.01
$a_{log,night}I_{day}$	−2.30	$a_{lin,evening}$	1.47
$a_{log,evening}a_{lin,night}$	−2.30	$a_{log,day}a_{log,night}$	1.66
$I_{evening}$	−2.28	$I_{day}I_{evening}$	1.90
$a_{log,day}a_{lin,night}$	−2.11	$a_{log,day}a_{lin,evening}$	2.40
$a_{lin,day}a_{log,night}$	−1.26	$a_{lin,day}$	2.48
$a_{log,day}I_{evening}$	−1.14	$a_{lin,evening}a_{lin,night}$	2.52
$a_{log,evening}$	−1.04	$a_{lin,night}I_{day}$	2.96
$a_{lin,evening}a_{log,night}$	−0.77	$a_{log,evening}a_{lin,evening}$	3.37
		$a_{log,day}a_{log,evening}$	3.73
		$a_{log,day}$	6.37
		$a_{log,day}a_{lin,day}$	7.83

Multiple linear regression analysis without interaction terms yields a reduced squared correlation coefficient of 53%. Including linear terms, interaction terms, together with the squares of the 9 base parameters, resulted in a model that explains 90% of the observed variability. It can therefore be concluded that the interaction terms are clearly relevant, while the inclusion of quadratic terms is only a minor improvement and would complicate further analysis.

The standardized coefficients of the independent variables allow one to make a ranking of the principal parameters. The use of t-tests helps to determine if an individual parameter or a pair-wise combination of parameters has predictive power. The null hypothesis, stating that a coefficient is equal to zero, must in that case be rejected at a very high statistical level. In our analysis, a 99.99% level is chosen. 27 parameters where retained to build the model, and are shown in Table II. When looking at the importance of these parameters, the following observations could be made:

- The meteorological parameters determine the error in the first place. The days on which large errors are observed, are quite independent of the traffic data. A negative correlation between the error and $a_{lin,night}$ and $a_{log,evening}$ is observed, while $a_{lin,evening}$, $a_{lin,day}$ and $a_{log,day}$ are positively correlated.
- The interaction terms between a_{lin} and a_{log} parameters, in the same period, are important and positively correlated. A continuously increasing or decreasing effective sound speed curve with height results in the largest errors. Sound speed curves containing upward and downward refracting parts decrease the error. This

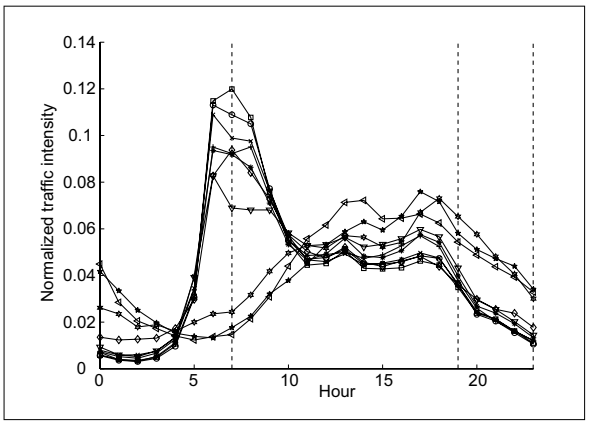

Figure 9. Top 10 normalized traffic intensity profiles resulting in the smallest errors, neglecting interactions with meteorological parameters. The vertical lines indicate night period, daytime period and evening period. Hour 10 means the period between 10.00h and 10.59h.

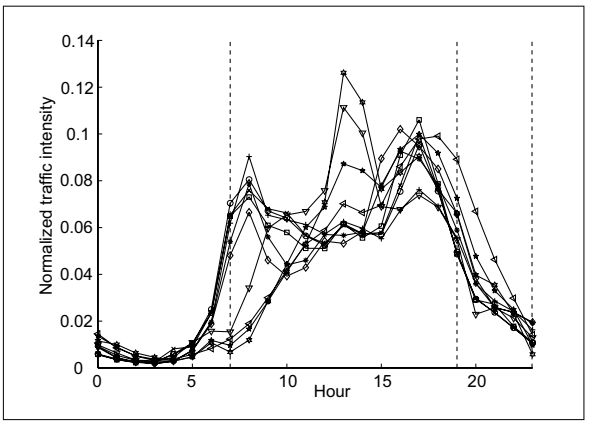

Figure 10. Top 10 normalized traffic intensity profiles resulting in the largest errors, neglecting interactions with meteorological parameters. The vertical lines indicate night period, daytime period and evening period. Hour 10 means the period between 10.00h and 10.59h.

effect is more pronounced during the day than during the evening or night.

- The interaction terms expressing meteorological conditions over successive periods in 24 hours are important. Important terms are $a_{\mathrm{log,evening}}$ combined with $a_{\mathrm{lin,night}}$, and $a_{\mathrm{log,evening}}$ combined with $a_{\mathrm{log,night}}$. An equal sign of these meteorological parameters in both periods decreases the error, while a change in sign yields larger errors. This is logical since a different sound propagation condition increases the error made when dividing up in separate periods. On the other hand, there are a number of positively correlated terms like $a_{\mathrm{log,day}}a_{\mathrm{log,evening}}$ and $a_{\mathrm{lin,night}}a_{\mathrm{lin,evening}}$ and $a_{\mathrm{log,day}}a_{\mathrm{lin,evening}}$. The standardized coefficients belonging to those combinations of parameters are smaller than the negatively correlated ones. The fact that there is a positive correlation may come from the large, positive influence that $a_{\mathrm{log,day}}$ exerts on the error.
- When considering pure traffic intensity terms, it is observed that large amounts of traffic during the evening tend to decrease the errors. The term $I_{\mathrm{day}}I_{\mathrm{evening}}$ on the other hand is positively correlated with the error: Large traffic intensities during both the day and the evening tend to increase the error. This also means that a large amount of traffic during the night decreases the error, since the sum of I_{day}, I_{evening}, and I_{night} equals 1. In Figures 9 and 10, the 10 traffic intensity profiles resulting in respectively the largest and smallest errors are shown, based on these findings.
- Pairs like $a_{\mathrm{night}}I_{\mathrm{night}}$ and $a_{\mathrm{evening}}I_{\mathrm{evening}}$ are less important than meteorological–traffic intensity pairs over different periods like $a_{\mathrm{night}}I_{\mathrm{day}}$ and $a_{\mathrm{day}}I_{\mathrm{evening}}$.

From this analysis, it is clear that the course of meteorological conditions over time influences the error introduced by using averaged information over day, evening and night period, the most. Selecting a subset of large-error days allowed confirming that the type of traffic intensity profile may intensify the error made by the averaging approach. The difference in error between various traffic intensity profiles on a single day can be as large as 10 dB(A).

It was shown by the multiple linear regression analysis that interaction terms, containing parameters of different periods, are important. The differences between approaches 1 or 2 and the reference calculation can therefore be considered as proportional to the variability in the a_{lin}–a_{log} pairs over time. On the other hand, when a_{lin}–a_{log} pairs stay more or less the same during the different hours of the day, the error by averaging over different periods is smallest. Such a small variability of meteorological conditions is typically observed during the winter period and in the case of a cloud-covered sky. During spring and summer, the strong solar radiation induces more distinct sound propagation conditions during the different periods of the day. Since multiple source points are used to represent the highway, quite different propagation conditions within a single meteorological observation are present, and this complicates this analysis. It can nevertheless be illustrated by looking at the spread of the a_{lin}–a_{log} pairs over time, for the days resulting in the largest and smallest errors. This is shown in Figures 11 and 12, respectively. A traffic intensity profile with a limited amount of traffic during the night and the evening was chosen. The use of such a_{lin}–a_{log} plots is helpful to estimate the importance of having detailed, temporal data.

6.2. Statistically-averaged meteorological data

The availability of a detailed meteorological dataset like the one used in this study, is rather uncommon. Therefore, an additional theoretical study on the accuracy of yearly averaged L_{den} based on statistically averaged meteo-data is conducted. Noise indicators using this approach are indicated with the subscript "STAT". Since it was shown in the previous sections that the effect of averaging on L_{den} and L_{night} is very similar, only L_{den} is considered. The fre-

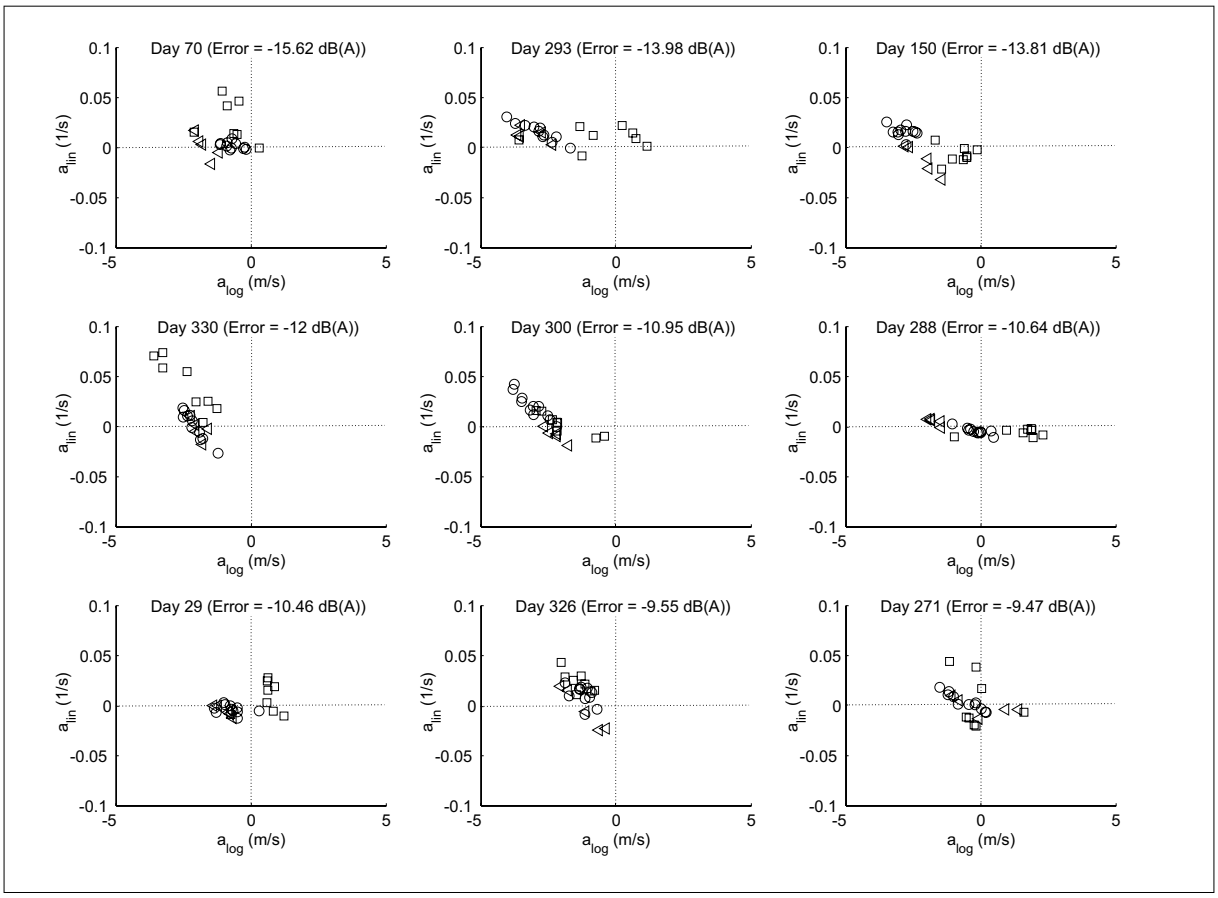

Figure 11. a_{lin}-a_{log} plots for the 9 days resulting in the largest errors on the one-day L_{den} indicator, when comparing approach 1 with the reference calculation ($= L^{(1)}_{\mathrm{den,1day,SEQ}} - L^{(\mathrm{ref})}_{\mathrm{den,1day,SEQ}}$). The hourly-averaged a_{lin}–a_{log} pairs are shown, for the source point closest to the receiver. The highway has a N-S orientation, and the receiver is located at 2 km in eastern direction. Day hours are indicated with the circles, evening hours with the triangles, and night hours with the squares. Day numbers range from 1 (First of January) to 365 (31 December).

quencies of occurrence over the year of the a_{lin}–a_{log} parameters are determined, using 25 classes. The class midpoints as suggested by the Harmonoise reference model [2] are used. For the a_{log} parameter, these are −1 m/s, −0.4 m/s, 0 m/s, 0.4 m/s, and 1 m/s. The class midpoints for the a_{lin} parameter are −0.12/s, −0.04/s, 0/s, 0.04/s, and 0.12/s.

Firstly, the frequencies in each class are calculated on an hourly basis. For each source-receiver combination, a different 5×5 frequency table is determined, leading to 10080 frequency tables (24 hours times 21 source points times 5 receivers times 4 configurations). Secondly, these frequencies are calculated for the day time, the evening time, and the night time period as a whole, leading to 1260 tables. Yearly-averaged hour-by-hour temperature and relative humidity is used in the first case. Yearly-averaged temperature and relative humidity over the 3 periods is used in the second case. The sound attenuation resulting from the 25 meteo-classes are weighted by their occurrence in time, instead of calculating them for each hour or period for each day separately throughout the year.

The most detailed approach based on statistical meteorological conditions, $L^{(\mathrm{ref})}_{\mathrm{den,1year,STAT}}$, now consists in combining hourly meteo-statistics with hour-by-hour traffic intensity profiles. Figure 13 shows $L^{(\mathrm{ref})}_{\mathrm{den,1year,STAT}} - L^{(\mathrm{ref})}_{\mathrm{den,1year,SEQ}}$. In a first further approximation, sound propagation calculations based on statically-averaged data over three periods are combined with traffic intensities for these 3 periods (*statistical approach 1*). Figure 14 shows $L^{(1)}_{\mathrm{den,1year,STAT}} - L^{(\mathrm{ref})}_{\mathrm{den,1year,SEQ}}$. A second approach assumes that only the total traffic intensity over 24 hours is known, and the GPG recommendations [19] are used to spread it over the three periods of the day (*statistical approach 2*). Figure 15 shows $L^{(2)}_{\mathrm{den,1year,STAT}} - L^{(\mathrm{ref})}_{\mathrm{den,1year,SEQ}}$. Note that as a reference for these representations, the most accurate predictions available are used, namely $L^{(\mathrm{ref})}_{\mathrm{den,1year,SEQ}}$, the (non-statistically) hour-by-hour attenuation calculations, using a very fine discretisation of the a_{lin}–a_{log} space (see section 3.1), in combination with hourly traffic intensities. The flow chart in Figure 4 gives a graphical overview of the different statistical calculation approaches mentioned.

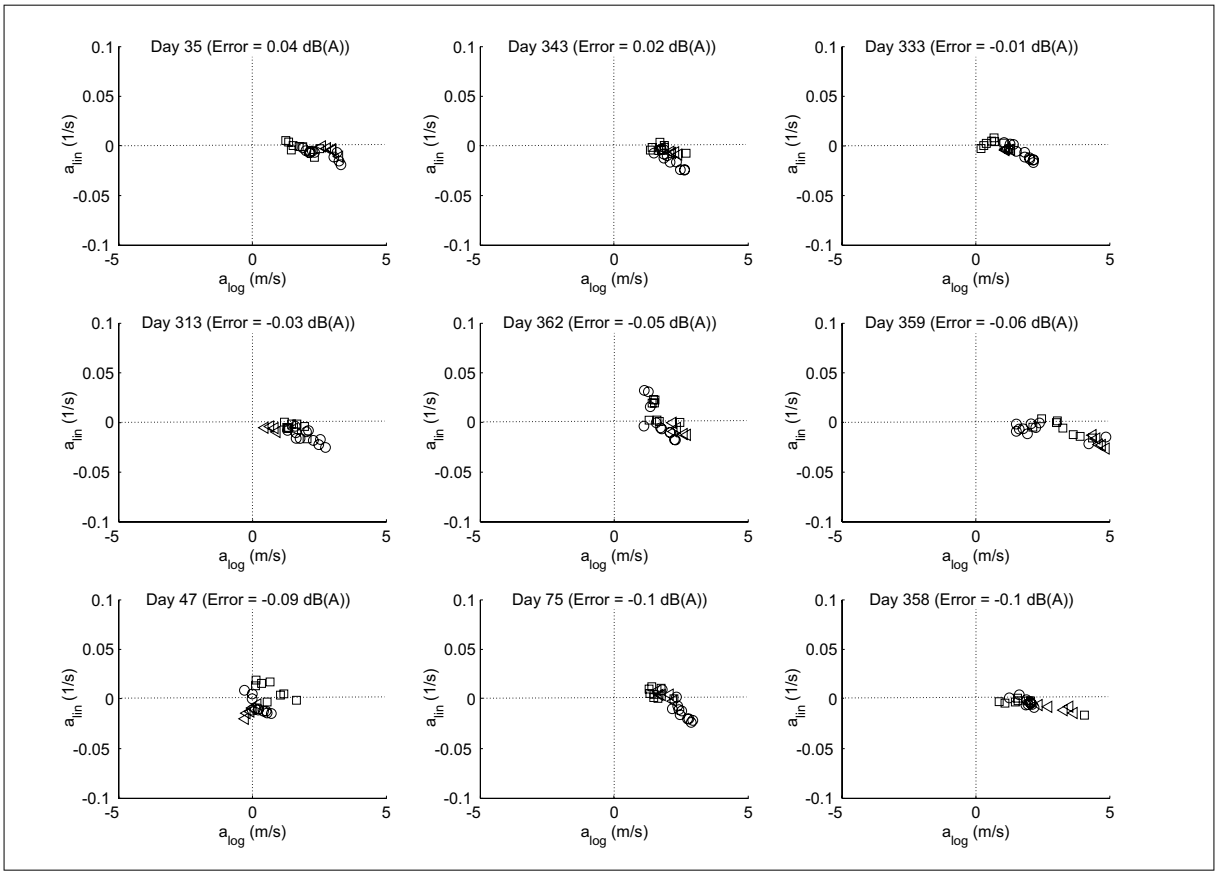

Figure 12. a_{lin}–a_{log} plots for the 9 days resulting in the smallest errors on the one-day L_{den} indicator, when comparing approach 1 with the reference calculation ($= L^{(1)}_{\mathrm{den,1day,SEQ}} - L^{(\mathrm{ref})}_{\mathrm{den,1day,SEQ}}$). The hourly-averaged a_{lin}–a_{log} pairs are shown, for the source point closest to the receiver. The highway has a N-S orientation, and the receiver is located at 2 km in eastern direction. Day time hours are indicated with the circles, evening hours with the triangles, and night hours with the squares. Day numbers range from 1 (First of January) to 365 (31 December).

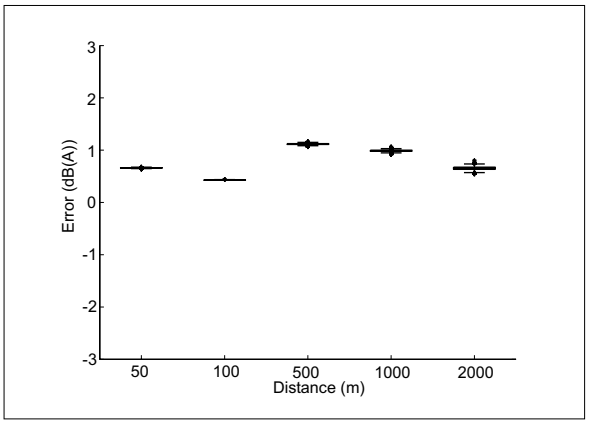

Figure 13. Errors on yearly L_{den} values by using statistical hour-by-hour calculations, relative to the reference calculation ($= L^{(\mathrm{ref})}_{\mathrm{den,1year,STAT}} - L^{(\mathrm{ref})}_{\mathrm{den,1year,SEQ}}$). The data points forming the box plots are the different traffic intensity profiles. The other configurations gave similar results and are therefore not shown.

The error introduced by statistically-averaged attenuation data on an hourly base, compared to the reference calculations, results in errors up to 1 dB(A) for yearly L_{den} values. Both calculation methods compared in Figure 13 account for the hourly correlation between traffic intensity and attenuation: The influence of the various traffic intensity profiles on this type of error is therefore very limited. An unambiguous trend between this error and the propagation distance is not observed. In [12] it is concluded that using 25 meteorological classes affects the calculation of yearly L_{den} with less than 2 dB(A). The smaller deviation found here might be the result of a mix of different propagation conditions within a single meteorological observation, since, in contrast to [12], a series of point sources is used here to represent a highway.

The additional error introduced by the averaging approach 1 (Figure 14) and 2 (Figure 15) does not increase the overall error more than in the case of non-statistical handling of meteorological conditions (Figure 6 and Figure 7). It simply adds up with the 1 dB(A) error observed in Figure 13. The spread of the error when using averaging approach 2 in the statistical approach is again larger than when using averaging approach 1. The underestimation increases with distance as well. It can therefore be concluded

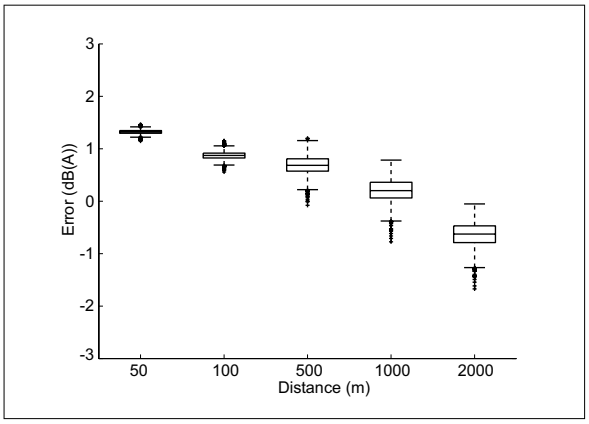

Figure 14. Errors on yearly L_{den} values by using the statistical approach 1, relative to the reference calculation ($= L^{(1)}_{\text{den,1year,STAT}} - L^{(\text{ref})}_{\text{den,1year,SEQ}}$). The data points forming the box plots are the different traffic intensity profiles. The other configurations gave similar results and are therefore not shown.

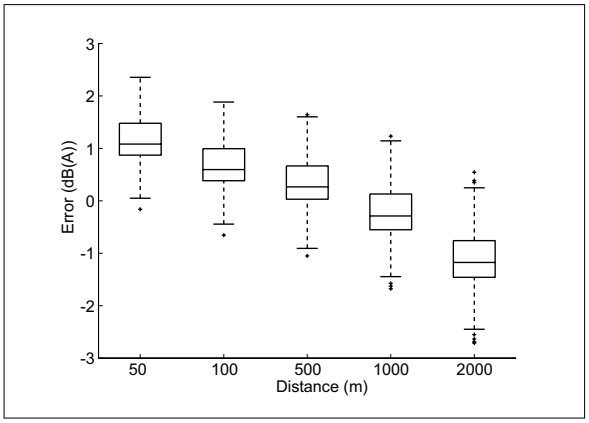

Figure 15. Errors on yearly L_{den} values by using the statistical approach 2, relative to the reference calculation ($= L^{(2)}_{\text{den,1year,STAT}} - L^{(\text{ref})}_{\text{den,1year,SEQ}}$). The data points forming the box plots are the different traffic intensity profiles. The other configurations gave similar results and are therefore not shown.

that applying statistically-averaged meteorological classes does not lead to an increased loss in accuracy when using the same temporal averaging approach.

7. Conclusions

In this paper, a theoretical study is conducted to investigate the impact of averaging approaches on meteorological conditions, on the course of traffic intensity over time, as well as on the temporal correlation between them. Focus is on the noise indicators L_{den} and L_{night}. The rationale behind this study is twofold: at one hand averaging prior to performing calculations may reduce the computational cost of noise mapping, at the other hand only average data may be available for example because traffic intensities are obtained from traffic simulations.

Highly detailed sound propagation calculations using the Green's Function Parabolic Equation method, accounting for refraction of sound by using meteorological data from a tower, are combined with state-of-the-art emission models to evaluate these indicators near a long straight highway.

Calculations that combine the emission at a certain hour with the corresponding attenuation for this same hour are taken as a reference. Periods with large traffic intensities and at the same time downward refracting sound propagation conditions contribute largely to L_{den} values. Not accounting for this temporal link in sufficient detail leads to average sound levels that are too low. When assuming that traffic data and sound attenuation data are known only as an average over the (default) day period, evening period and night period, large underestimations, up to 15 dB(A), are possible for one-day L_{den} predictions. When, in addition, daily traffic intensity is divided over day, evening and night using fixed fractions, the maximum error found increases further to 20 dB(A). The error increases with the sound propagation distance.

When considering an integration period of one year, the underestimation decreases considerably, and maximum errors are limited to 1.5 dB(A) and 3 dB(A) respectively. The error on L_{night} is very similar to the error on the L_{den} indicator, when using a similar averaging approach over time.

The meteorological parameters, and their course over time, determine the error caused by the averaging approaches in first place. The type of traffic intensity profile may intensify the errors made with 10 dB(A). A linear regression model, based on 9 parameters, was build to find the important actors during high-error days. These parameters are the fraction of traffic intensity during day time, evening time and night time, and the averages of the meteorological parameters a_{lin} and $a_{\log}$ during these 3 periods. When including interaction terms, 84% of the variability on the data can be explained. A ranking of the standardized parameters was made to estimate the influence of the parameters and their combinations on the errors made by the averaging approaches.

Interaction terms expressing meteorological conditions over successive periods in 24 hours are shown to be important, and are positively or negatively correlated with the error. Large (relative) amounts of traffic during the evening and night tend to decrease the error. Continuously increasing or decreasing effective sound speed profiles ($a_{\log}$ and a_{lin} have the same sign) result in larger errors than mixed profiles ($a_{\log}$ and a_{lin} have a different sign).

The error made by the averaging approaches is proportional to the variability of the hourly a_{lin}–$a_{\log}$ pairs during a 24 hour period. The use of a_{lin}–$a_{\log}$ plots could be used as a quick and easy way to estimate the detail needed in temporal data to calculate short-term L_{den} values. It is expected that the required detail will be lower during winter time than during summer time.

The use of meteorological data, statistically-averaged over the year, results in a loss of accuracy smaller than

2 dB(A), compared to calculating noise levels for each hour of the year, and averaging results afterwards. The additional error introduced by the approach to average meteorological data and traffic intensity over the day is not affected by using statistically-averaged yearly meteo data.

It should be noted that the quantitative results obtained in this study only apply for locations with similar meteorological statistics as in this study, and for sound propagation over a flat terrain. Nevertheless, the numerical values obtained are indicative for potential trends.

References

[1] Review of data needs for road noise source modelling. IMAGINE Technical report IMA2TR-040615-M+P10, 2004.

[2] J. Defrance, E. Salomons, I. Noordhoek, D. Heimann, B. Plovsing, G. Watts, H. Jonasson, X. Zhang, E. Premat, I. Schmich, F. Aballea, M. Baulac, F. de Roo: Outdoor sound propagation reference model developed in the European Harmonoise project. Acta Acustica united with Acustica **93** (2007) 213–227.

[3] T. Van Renterghem, D. Botteldooren: Influence of correlation between diurnal traffic pattern and meteorological conditions on long-term average L_{den}. Proceedings of Euronoise, Tampere, Finland, 2006.

[4] ISO 9613-1: Acoustics – attenuation of sound during propagation outdoors – Part 1. International Organisation for Standardisation, Geneva, Switzerland, 1996.

[5] H. Jonasson: Acoustical source modelling of road vehicles. Acta Acustica united with Acustica **93** (2007) 173–184.

[6] K. Gilbert, X. Di: A fast Green's function method for one-way sound propagation in the atmosphere. J. Acoust. Soc. Am. **94** (1993) 2343–2352.

[7] E. Salomons: Improved Green's function parabolic equation method for atmospheric sound propagation. J. Acoust. Soc. Am. **104** (1998) 100–111.

[8] M. Delany, E. Bazley: Acoustic properties of fibrous absorbent materials. Appl. Acoust. **3** (1970) 105–116.

[9] J. Cooper, D. Swanson: Parameter selection in the Green's function parabolic equation. Appl. Acoust. **68** (2007) 390–402.

[10] E. Salomons: Computational atmospheric acoustics. Kluwer, Dordrecht, The Netherlands, 2001.

[11] D. Heimann, M. Bakermans, J. Defrance, D. Kühner: Vertical sound speed profiles determined from meteorological measurements near the ground. Acta Acustica united with Acustica **93** (2007) 228–240.

[12] D. Heimann, E. Salomons: Testing meteorological classifications for the prediction of long-term average sound levels. Appl. Acoust. **65** (2004) 925–950.

[13] A. Cramond, C. Don: Effects of moisture content on soil impedance. J. Acoust. Soc. Am. **82** (1987) 293–301.

[14] K. Horoshenkov, M. Mohamed: Experimental investigation of the effects of water saturation on the acoustic admittance of sandy soils. J. Acoust. Soc. Am. **120** (2006) 1910–1921.

[15] E. Salomons, V. Ostashev, S. Clifford, R. Lataitis: Sound propagation in a turbulent atmosphere near the ground: An approach based on the spectral representation of refractive-index fluctuations. J. Acoust. Soc. Am. **109** (2001) 1881–1893.

[16] X. Di, K. Gilbert, L. Ameling: A fast phase-screen method for sound propagation through a turbulent atmosphere. J. Acoust. Soc. Am. **93** (1993) 2407.

[17] F. Wiener, D. Keast: Experimental study of the propagation of sound over ground. J. Acoust. Soc. Am. **31** (1959) 724–733.

[18] P. Chevret, P. Blanc-Benon, D. Juve: A numerical model for sound propagation through a turbulent atmosphere near the ground. J. Acoust. Soc. Am. **100** (1996) 3587–3599.

[19] European Commission Working Group Assessment of Exposure to Noise (WG-AEN): Good practice guide for strategic noise mapping and the production of associated data on noise exposure. Technical report, 2004.